Particle Flow Calorimetry

Journal of Physics: Conference Series **293** (2011) 012021 doi:10.1088/1742-6596/293/1/012021

Particle Flow Calorimetry

Mark A. Thomson

University of Cambridge, Cavendish Laboratory, JJ Thomson Avenue, Cambridge CB3 0HE, UK

E-mail: thomson@hep.phy.cam.ac.uk

Abstract. The Particle Flow (PFlow) approach to calorimetry promises to deliver unprecedented jet energy resolution for experiments at future high energy colliders such as the proposed International Linear Collider (ILC). Since Calor 2008 there has been a significant improvement in understanding particle flow calorimetry and its potential. This contribution to the proceedings describes the current understanding of high granularity particle flow calorimetry in the context of the PandoraPFA algorithm and the ILD detector concept. It is shown that a jet energy resolution of $\sigma_E/E \lesssim 4\,\%$ is achievable for $40-400\,\mathrm{GeV}$ jets, demonstrating that high granularity PFlow calorimetry can meet the challenging ILC jet energy resolution goals. The potential of high granularity PFlow calorimetry at a multi-TeV lepton collider, such as CLIC and a possible Muon Collider, is also discussed.

1. Introduction

In recent years the concept of high granularity Particle Flow calorimetry [1, 2] has been developed in the context of the proposed International Linear Collider (ILC) [4]. The goal for jet energy resolution at the ILC is that it is at least sufficient to cleanly separate W and Z hadronic decays; an invariant mass resolution comparable to the gauge boson widths, i.e. $\sigma_m/m = 2.7\,\% \approx \Gamma_W/m_W \approx \Gamma_Z/m_Z$, leads to an effective $2.5\,\sigma$ separation of the $\mathrm{W} \to \mathrm{q}'\overline{\mathrm{q}}$ and $\mathrm{Z} \to \mathrm{q}\overline{\mathrm{q}}$ mass peaks. It is only recently that it is been demonstrated that this level of performance can be achieved with Particle Flow Calorimetry [3].

In the traditional calorimetric approach, the jet energy is obtained from the sum of the energies deposited in the electromagnetic and hadronic calorimeters (ECAL and HCAL). This typically results in a jet energy resolution of the form

$$\frac{\sigma_E}{E} \;=\; \frac{\alpha}{\sqrt{\mathrm{E(GeV)}}} \oplus \beta.$$

The stochastic term, α, is usually greater than $\sim$50 % and the constant term, β, which encompasses a number of effects, is typically a few per cent. The stochastic term alone results in a contribution to the di-jet mass resolution of $\sigma_m/m \approx \alpha/\sqrt{E_{jj}}$, where E_{jj} is the energy of the di-jet system in GeV. At the ILC, operating at centre-of-mass energies $\sqrt{s} = 0.5 - 1.0\,\mathrm{TeV}$, the typical di-jet energies will be in the range $150 - 350\,\mathrm{GeV}$. Even if one neglects the constant term, to achieve the ILC goal of $\sigma_m/m = 2.7\,\%$, the stochastic term must be $\lesssim 30\,\%/\sqrt{\mathrm{E(GeV)}}$. This is unlikely to be achievable with a traditional approach to calorimetry.

1.1. The Particle Flow Approach to Calorimetry

On average, 62% of the jet energy is carried by charged particles (mainly hadrons), around 27% by photons, about 10% by long-lived neutral hadrons (e.g. n, $\overline{n}$ and $K_{\rm L}$), and around 1.5 % by neutrinos. Hence, approximately 72 % of the jet energy is measured with the precision of the combined ECAL and HCAL for hadrons; the jet energy resolution is thus limited by the relatively poor hadronic energy resolution, typically $\gtrsim 50\,\%/\sqrt{\rm E(GeV)}$. A number of collider experiments (e.g. OPAL, H1 and D0) obtained improved jet energy resolution using the Energy Flow approach, whereby energy deposits in the calorimeters are removed according to the momentum of associated charged particle tracks. ALEPH [5] used particle flow techniques to attempt to reconstruct the four momenta of the particles in an event. However, due to the relatively low granularity of the calorimeters, energy depositions from neutral hadrons still had to be identified as a significant excesses of calorimetric energy compared to the associated charged particle tracks. Nevertheless, ALEPH achieved a jet energy resolution (for $\sqrt{s} = M_{\rm Z}$) equivalent to $\sigma_E = (59\,\%\sqrt{E/\rm GeV} + 0.6)\,\rm GeV$ [5], roughly a factor two worse than required for the ILC even for these relatively low energy jets.

Within the ILC community it is believed that the most promising strategy for achieving the ILC jet energy goal is the Particle Flow (PFlow) approach to calorimetry using a *highly granular* detector. In contrast to a purely calorimetric measurement, PFlow calorimetry requires the reconstruction of the four-vectors of all visible particles in an event. The reconstructed jet energy is the sum of the energies of the individual particles. The momenta of charged particles are measured in the tracking detectors, while the energy measurements for photons and neutral hadrons are obtained from the calorimeters. In this manner, the HCAL is used to measure only $\sim 10\,\%$ of the energy in the jet. If one were to assume calorimeter resolutions of $\sigma_E/E = 0.15/\sqrt{\rm E(GeV)}$ for photons and $\sigma_E/E = 0.55\sqrt{\rm E(GeV)}$ for hadrons, a jet energy resolution of $0.19/\sqrt{\rm E(GeV)}$ would be obtained with the contributions from tracks, photons and neutral hadrons as given in Table 1. In practice, this level of performance can not be achieved as it is not possible to perfectly associate all energy deposits with the correct particles. For example, if the calorimeter hits from a photon are not resolved from a charged hadron shower, the photon energy is not accounted for. Similarly, if part of charged hadron shower is identified as a separate cluster, the energy is effectively double-counted as it is already accounted for by the track momentum. This *confusion* rather than calorimetric performance is the limiting factor in PFlow calorimetry. Thus, the crucial aspect of PFlow calorimetry is the ability to correctly assign calorimeter energy deposits to the correct reconstructed particles, placing stringent requirements on the granularity of the ECAL and HCAL. For the jet energy reconstruction, the sum of calorimeter energies is replaced by a complex pattern recognition problem, namely the Particle Flow reconstruction Algorithm (PFA). The jet energy resolution obtained is a combination of the intrinsic detector performance and the performance of the PFA software. The PandoraPFA algorithm[3] was developed to study PFlow calorimetry at the ILC and represents the state-of-the-art in high granularity PFlow reconstruction.

Component	**Detector**	**Energy Fract.**	**Energy Res.**	**Jet Energy Res.**
Charged Particles ($X^{\pm}$)	Tracker	$\sim 0.6\,E_j$	$10^{-4}\,E^2_{X^{\pm}}$	$< 3.6 \times 10^{-5}\,E_j^2$
Photons (γ)	ECAL	$\sim 0.3\,E_j$	$0.15\,\sqrt{E_\gamma}$	$0.08\,\sqrt{E_j}$
Neutral Hadrons (h^0)	HCAL	$\sim 0.1\,E_j$	$0.55\,\sqrt{E_{h^0}}$	$0.17\,\sqrt{E_j}$

Table 1. Contributions from the different particle components to the jet-energy resolution (all energies in GeV). The table lists the approximate fractions of charged particles, photons and neutral hadrons in a jet of energy, E_j, and the assumed single particle energy resolution.

It is important to realise that PFlow calorimetry is very different from the traditional approach, the aim is to use the energies measured in the calorimeters as little as possible. The accepted wisdom for calorimetry may not hold for particle flow calorimetry as it is a very different technique.

2. Overview a Particle Flow Detector

The studies presented in this contribution were performed in the context of the Geant4 [7] simulation of the ILD detector concept [8]. It consists of a vertex detector, tracking detectors, ECAL, HCAL and muon chambers. For the ECAL and HCAL the emphasis is on granularity, both longitudinal and transverse, rather than solely energy resolution. Suitable candidate technologies are being studied by the CALICE (calorimetry for the ILC) collaboration [9]. Amongst these are the Silicon-Tungsten ECAL and Steel-Scintillator HCAL designs assumed for the ILD reference detector simulation. The R&D and detector prototyping performed within the CALICE collaboration (described elsewhere in these proceedings) has reached the point where one can be confident that such a detector ultimately could be constructed.

In the ILD concept, both the ECAL and HCAL are located inside a solenoid which is taken to produce the 3.5 T magnetic field. The main tracking detector is simulated as a time projection chamber (TPC) with an active gas volume of half-length 2.25 m and inner and outer radii of 0.39 m and 1.74 m respectively. The ECAL is simulated as a Silicon-Tungsten sampling calorimeter consisting of 29 layers. The first 20 layers have 2.1 mm thick Tungsten and the last 9 layers have 4.2 mm thick Tungsten. The high resistivity Silicon is segmented into $5 \times 5\,\mathrm{mm}^2$ pixels. At normal incidence, the ECAL corresponds to 23 radiation lengths (X_0) and 0.8 nuclear interaction lengths (λ_I). The HCAL is simulated as a Steel-Scintillator sampling calorimeter comprising 48 layers of 20 mm thick Steel and 5 mm thick $3 \times 3\,\mathrm{cm}^2$ plastic scintillator tiles. At normal incidence the HCAL is $6\,\lambda_I$ thick.

The ECAL and HCAL in the ILD concept are well matched to the requirements of PFlow calorimetry. Tungsten is the ideal absorber material for the ECAL; it has a short radiation length and small Molière radius which leads to compact electromagnetic (EM) showers. It also has a large ratio of interaction length to radiation length which means that hadronic showers will tend to be longitudinally well separated from EM showers. The $5 \times 5\,\mathrm{mm}^2$ transverse segmentation takes full advantage of the small Molière radius. Steel is chosen as the HCAL absorber, primarily for its structural properties. The $3 \times 3\,\mathrm{cm}^2$ HCAL transverse segmentation is well matched to the requirements of PFlow calorimetry.

The performance of PFlow calorimetry depends strongly on the reconstruction software. For the results obtained to be meaningful, it is essential that both the detector simulation and the reconstruction chain are as realistic as possible. For this reason no Monte Carlo (MC) information is used at any stage in the reconstruction as this is likely to lead to an overly-optimistic evaluation of the potential performance of PFlow calorimetry. PandoraPFA runs in the MARLIN [6] C++ framework developed for the LDC and ILD detector concepts. Tracks in the TPC are reconstructed using TPC pattern recognition software [10] based on that used by ALEPH and track fitting software used by DELPHI [11]. PandoraPFA combines the tracking information with hits in the high granularity calorimeters to reconstruct the individual particles in the event. As an example of the information used in the reconstruction, Figure 1 shows a photon, a charged hadron (π^+) and a neutral hadron (K_L) as simulated in the ILD detector concept.

3. The PandoraPFA Particle Flow Algorithm

The PandoraPFA algorithm is described in detail in [3] and only an overview is presented here. It is a complex reconstruction programme with a number of distinct stages: *1) Track Selection/Topology:* track topologies such as kinks and decays of neutral particles in the detector

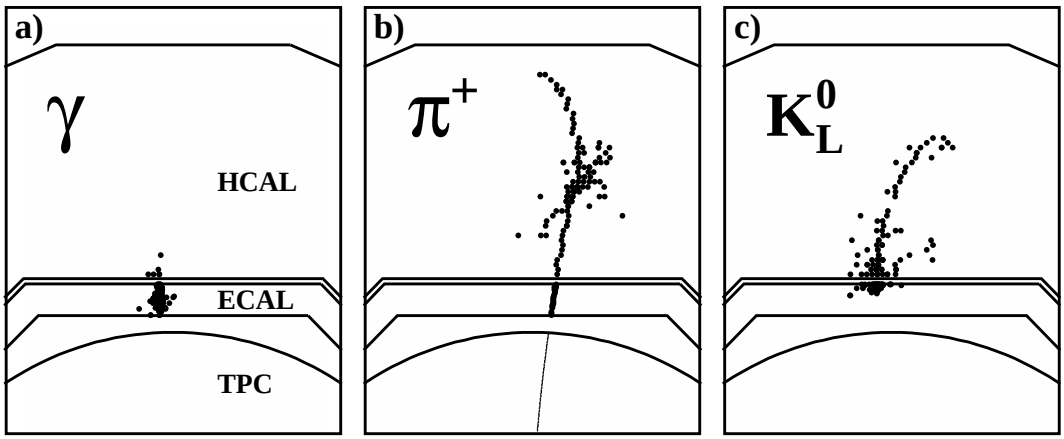

Figure 1. Example simulated single particle interactions in the ILD detector concept: a) a 10 GeV photon; b) a 10 GeV π^+ and c) a 10 GeV K_{L}. Hits in the TPC, ECAL and HCAL are shown. For the ECAL (HCAL) all hits with energy depositions $> 0.5\,(0.3)$ minimum ionising particle equivalent are displayed. Simulated TPC hits are digitised assuming 227 radial rows of readout pads.

volume (*e.g* $K_{\mathrm{S}} \rightarrow \pi^+\pi^-$) are identified. *2) Calorimeter Hit Selection and Ordering:* isolated hits, defined on the basis of proximity to other hits, are removed from the initial clustering stage. The remaining hits are ordered into *pseudo-layers* and information related to the geometry and the surrounding hits are stored for use in the reconstruction. *3) Clustering:* the main clustering algorithm is a cone-based forward projective method [12] working from innermost to outermost pseudo-layer. The algorithm starts by seeding clusters using the projections of reconstructed tracks onto the front face of the ECAL. *3A) Photon Clustering:* PandoraPFA can be run in a mode where the above clustering algorithm is performed in two stages. In the first stage, only ECAL hits are considered with the aim of identifying energy deposits from photons. In the second stage the clustering algorithm is applied to the remaining hits. *4) Topological Cluster Merging:* by design the initial clustering stage errs on the side of splitting up true clusters rather than merging energy deposits from more than one particle into a single cluster. Clusters are then combined on the basis of clear topological signatures in the high granularity calorimeters. The topological cluster merging algorithms are only applied to clusters which have not been identified as photons. *5) Statistical Re-clustering:* The previous four stages of the algorithm are found to perform well for jets with energies of less than 50 GeV. For higher energy jets the performance degrades due to the increasing overlap between hadronic showers from different particles. Clusters which are likely to have been created from the merging of hits in showers from more than one particle are identified on the basis of the compatibility of the cluster energy, E_C, and the associated track momentum, p. In the case of an inconsistent energy-momentum match, attempts are made to re-cluster the hits by re-applying the clustering algorithm with different parameters, until the cluster splits to give a cluster energy consistent with the momentum of the associated track. *6) Photon Recovery and Identification:* A more sophisticated, shower-profile based, photon-identification algorithm is then applied to the clusters, improving the tagging of photons. It is also used to recover cases where a primary photon is merged with a hadronic shower from a charged particle. *7) Fragment Removal:* "neutral clusters" which are *fragments* of charged particle hadronic showers are identified. *8) Formation of Particle Flow Objects:* The final stage of the algorithm is to create the list of reconstructed particles, Particle Flow Objects (PFOs), and associated four-momenta.

4. Parametrising Particle Flow Performance: rms_{90}

Figure 2 shows the distribution of PFA reconstructed energy for simulated $(\mathrm{Z}/\gamma)^* \rightarrow \mathrm{q\overline{q}}$ events (light quarks only, i.e. q=u,d,s) generated at $\sqrt{s} = 200\,\mathrm{GeV}$ with the Z decaying at rest, termed "$\mathrm{Z} \rightarrow$ uds" events. A cut on the polar angle of the generated $\mathrm{q\overline{q}}$ system, $\theta_{\mathrm{q\overline{q}}}$, is chosen to avoid the barrel/endcap overlap region, $|\cos\theta_{\mathrm{q\overline{q}}}| < 0.7$. Only light quark decays are considered here as, currently, PandoraPFA does not include specific reconstruction algorithms to attempt to recover missing energy from semi-leptonic decays of heavy quarks.

It is essential to realise that the reconstructed energy distribution of Figure 2 is not Gaussian. This is not surprising; one might expect a Gaussian core for perfectly reconstructed events (where the calorimetric energy resolution for hadrons dominates), and tails corresponding to the population of events where confusion is significant. Quoting the rms, in this case 5.8 GeV, as a measure of the jet energy resolution makes little sense as it over-emphasises the importance of these tails. In order to quote the energy resolution a more robust estimator than the raw rms is required. The chosen measure, rms_{90}, is defined as the rms in the smallest range of reconstructed energy which contains 90 % of the events. For the reconstructed data shown in Figure 2, $\mathrm{rms}_{90} = 4.1\,\mathrm{GeV}$ (equivalent to a single jet energy resolution of 2.9 %). The advantage of using rms_{90} is that it is robust and is relatively insensitive to the tails of the distribution; it parametrises the resolution for the bulk of the data.

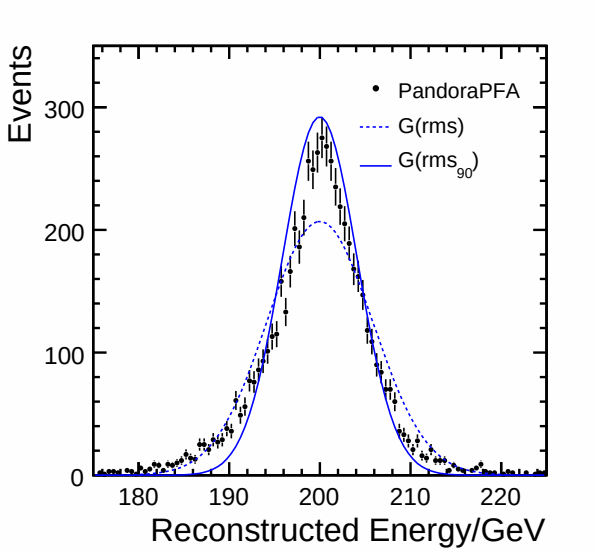

Figure 2. The total reconstructed energy from reconstructed PFOs in 200 GeV $\mathrm{Z} \rightarrow$ uds events for initial quark directions within the polar angle acceptance $|\cos\theta_{\mathrm{q\overline{q}}}| < 0.7$. The dotted line shows the best fit Gaussian distribution with an rms of 5.8 GeV. The solid line shows a Gaussian distribution, normalised to the same number of events, with standard deviation equal to rms_{90} (i.e. $\sigma = 4.1\,\mathrm{GeV}$).

A possible criticism [17] of the use of rms_{90} is that for a Gaussian distribution, rms_{90} is 21 % smaller than the true rms and thus significantly underestimates the true resolution. This misses the point. Unless the confusion term is eliminated, the PFA reconstructed jet energy distribution will never be Gaussian. For a non-Gaussian distribution the rms is not necessarily a good measure of the *analysing power* of a measurement. The equivalent Gaussian statistical analysing power, obtained from a MC study [3], shows that for the PandoraPFA reconstruction, rms_{90} is equivalent to a Gaussian resolution with $\sigma = 1.1 \times \mathrm{rms}_{90}$. Hence whilst rms_{90} does

underestimate the resolution (in terms of equivalent analysing power), it is only a 10 % effect relative to a pure Gaussian distribution. It should be noted that quoting the raw rms of the PFlow reconstructed distribution over-estimates the equivalent analysing power by 30 %.

5. Particle Flow Performance

Jet Energy	**rms**	$\mathbf{rms_{90}}(E_{jj})$	$\mathbf{rms_{90}}(E_{jj})/\sqrt{E_{jj}}$	$\mathbf{rms_{90}}(E_j)/E_j$
45 GeV	3.4 GeV	2.4 GeV	25.2 %	(3.74 ± 0.05) %
100 GeV	5.8 GeV	4.1 GeV	29.2 %	(2.92 ± 0.04) %
180 GeV	11.6 GeV	7.6 GeV	40.3 %	(3.00 ± 0.04) %
250 GeV	16.4 GeV	11.0 GeV	49.3 %	(3.11 ± 0.05) %
375 GeV	29.1 GeV	19.2 GeV	81.4 %	(3.64 ± 0.05) %
500 GeV	43.3 GeV	28.6 GeV	91.6 %	(4.09 ± 0.07) %

Table 2. Jet energy resolution for Z →uds events with $|\cos\theta_{q\overline{q}}| < 0.7$, expressed as: i) the rms of the reconstructed di-jet energy distribution, E_{jj}; ii) rms_{90} for E_{jj}; iii) the effective constant α in $\mathrm{rms}_{90}(E_{jj})/E_{jj} = \alpha(E_{jj})/\sqrt{E_{jj}(\mathrm{GeV})}$; and iv) the fractional jet energy resolution for a single jet where $\mathrm{rms}_{90}(E_j) = \mathrm{rms}_{90}(E_{jj})/\sqrt{2}$.

The performance of the PandoraPFA algorithm with the ILD detector concept was studied using MC samples of approximately 10000 $Z \to uds$ generated with the Z decaying at rest with E_Z = 91.2, 200, 360, and 500 GeV. These jet energies are typical of those expected at the ILC operating at $\sqrt{s} = 0.5 - 1.0$ TeV. In addition, to study the performance at higher energies, events were generated with E_Z = 750 GeV and 1 TeV. Jet fragmentation and hadronisation was performed using the PYTHIA [13] program tuned to the fragmentation data from the OPAL experiment [14]. The events were passed through the MOKKA simulation of the ILD detector concept which is described in detail in [8]. The `LCPHYS`[16] Geant4 physics list was used for the modelling of hadronic showers. For each set of events, the total energy is reconstructed and the jet energy resolution is obtained by dividing the total energy resolution by $\sqrt{2}$. Figure 3 shows the jet energy resolution as a function of the polar angle of the quarks in $Z \to q\overline{q}$ events. The energy resolution does not vary significantly in the region $|\cos\theta| < 0.975$. A small degradation in the energy resolution is seen for the barrel-endcap overlap region, $0.7 < |\cos\theta| < 0.8$. In addition, there is a small degradation in performance at $\cos\theta \approx 0$ due to the TPC central membrane and gaps between sections of the HCAL as simulated in the ILD detector model.

Table 2 summarises the current performance of the PandoraPFA algorithm applied to ILD detector simulation. For the typical ILC jet energy range, $45 - 250$ GeV, the energy resolution is significantly better than the best resolution achieved at LEP, $\sigma_E/E \approx 0.65/\sqrt{E(\mathrm{GeV})}$. Table 2 also lists the single jet energy resolution. For jet energies in the range $45 - 375$ GeV this is better than 3.8 %, which is necessary to resolve hadronic decays of W and Z bosons. These results clearly demonstrate the potential of PFlow calorimetry at the ILC; the jet energy resolution obtained is approximately a factor two better than might be achievable with a traditional calorimetric approach. Furthermore, it is expected that the performance of PandoraPFA will improve with future refinements to the algorithm.

It is worth noting, that for perfect PFlow reconstruction, the energy resolution would be described by $\sigma_E/E \approx \alpha/\sqrt{\mathrm{E(GeV)}}$, where α is a constant. The fact that this does not apply is no surprise; as the particle density increases it becomes harder to correctly associate the calorimetric energy deposits to the particles and the confusion term increases.

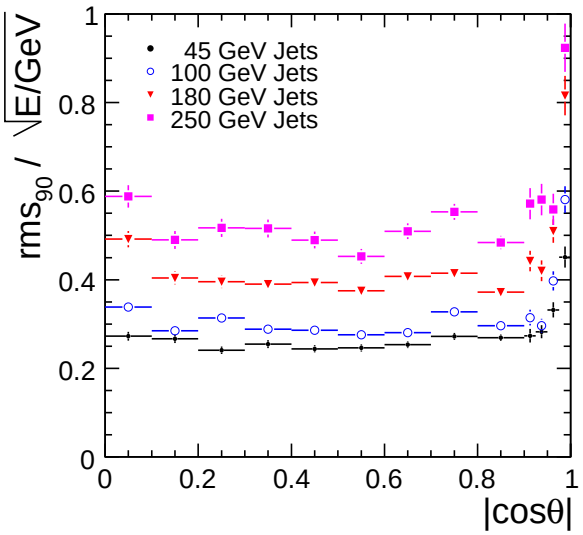

Figure 3. The jet energy resolution, defined as the α in $\sigma_E/E = \alpha/\sqrt{\mathrm{E(GeV)}}$, plotted versus $\cos\theta_{\mathrm{q\overline{q}}}$ for four different values of $\sqrt{s}$. The plot shows the resolution obtained from $(\mathrm{Z}/\gamma)^* \rightarrow \mathrm{q\overline{q}}$ events (q=u,d,s) generated at rest.

6. Understanding Particle Flow Performance

PandoraPFA is a fairly complex algorithm with a number of distinct stages which interact with each other in the sense that reconstruction failures in one part of the software can be corrected at a later stage. The contributions to the jet energy resolution have been estimated empirically by replacing different steps in PandoraPFA with algorithms which use MC information to perform: a) perfect reconstruction of photons as the first phase of the algorithm; b) perfect reconstruction of neutral hadrons; and c) perfect identification of fragments from charged hadrons. The jet energy resolutions obtained using these "perfect" algorithms enable the contributions from *confusion* to be estimated. In addition, studies using a deep HCAL enable the contribution from leakage to be estimated. Finally, MC information can be used to perform ideal track pattern recognition enabling the impact of imperfect track finding code to be assessed. For the current PandoraPFA algorithm, the contribution from the calorimetric energy resolution, $\approx 21\,\%/\sqrt{E}$, dominates the jet energy resolution for 45 GeV jets. For higher energy jets, the confusion term dominates. This behaviour is summarised in Figure 4. The contributions from resolution and confusion are roughly equal for 120 GeV jets. The most important contribution for high energy jets is confusion due to neutral hadrons being lost within charged hadron showers.

From the above study it is possible to obtain an semi-empirical parametrisation of the jet energy resolution:

$$\frac{\mathrm{rms_{90}}}{E} = \frac{21}{\sqrt{E}} \oplus 0.7 \oplus 0.004E \oplus 2.1\left(\frac{E}{100}\right)^{0.3}\ \%,$$

where E is the jet energy in GeV. The four terms in the expression respectively represent: the intrinsic calorimetric resolution; imperfect tracking; leakage and confusion. For a significant range of the jet energies relevant for the ILC, *high granularity* PFlow results in a jet energy resolution which is roughly a factor two better than the best achieved at LEP ($\sigma_E/E = 6.8\,\%$ at $\sqrt{s} = M_{\mathrm{Z}}$). The ILC jet energy goal of $\sigma_E/E < 3.8\,\%$ is reached in the jet energy range 40 GeV − 420 GeV. Due to the confusion term, the performance of particle flow calorimetry, can not be

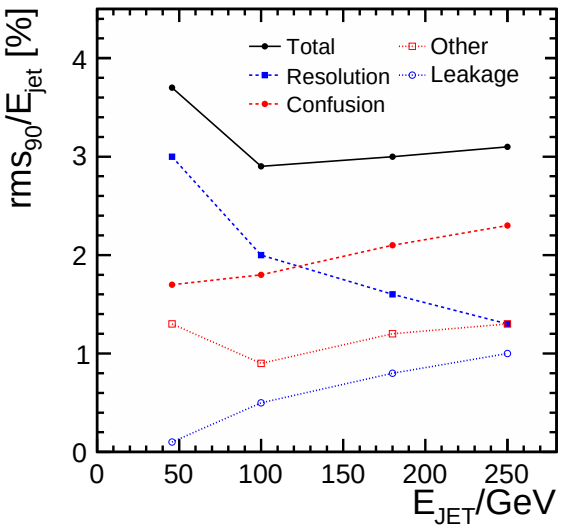

Figure 4. The contributions to the PFlow jet energy resolution obtained with PandoraPFA as a function of energy. The total is (approximately) the quadrature sum of the components.

expressed in the form $\sigma_E/E = \alpha/\sqrt{\mathrm{E(GeV)}} \oplus \beta$. Nevertheless, for comparison with traditional calorimetric approaches it is worth noting that for jets of energy less than 250 GeV a reasonable approximation of the *Gaussian equivalent* performance is:

$$\frac{\sigma}{E} \quad < \quad \frac{23\,\%}{\sqrt{E}} \oplus 3.0\,\%.$$

7. Dependence on Hadron Shower Modelling

Physics List	**Jet Energy Resolution $r = \mathrm{rms}_{90}(E_j)/E_j$**			
	45 GeV	100 GeV	180 GeV	250 GeV
`LCPhys`	$(3.74 \pm 0.05)\,\%$	$(2.92 \pm 0.04)\,\%$	$(3.00 \pm 0.04)\,\%$	$(3.11 \pm 0.05)\,\%$
`QGSP_BERT`	$(3.52 \pm 0.06)\,\%$	$(2.95 \pm 0.06)\,\%$	$(2.98 \pm 0.06)\,\%$	$(3.25 \pm 0.07)\,\%$
`QGS_BIC`	$(3.51 \pm 0.06)\,\%$	$(2.89 \pm 0.05)\,\%$	$(3.12 \pm 0.07)\,\%$	$(3.20 \pm 0.07)\,\%$
`FTFP_BERT`	$(3.68 \pm 0.08)\,\%$	$(3.10 \pm 0.06)\,\%$	$(3.24 \pm 0.06)\,\%$	$(3.26 \pm 0.08)\,\%$
`LHEP`	$(3.87 \pm 0.07)\,\%$	$(3.15 \pm 0.06)\,\%$	$(3.16 \pm 0.06)\,\%$	$(3.08 \pm 0.06)\,\%$
χ^2 (4 d.o.f)	23.3	17.8	16.0	6.3
rms/mean ($\sigma_r/\overline{r}$)	4.2 %	3.9 %	3.5 %	2.5 %

Table 3. Comparison of the jet energy resolution obtained using different hadronic shower physics lists. The χ^2 consistency of the different models for each jet energy are given as are the rms variations between the five models.

The results of the above studies rely on the accuracy of the MC simulation in describing EM and hadronic showers. The Geant4 MC provides a good description of EM showers as has been demonstrated in a series of test-beam experiments [15] using a Silicon-Tungsten ECAL of the type assumed for the ILD detector model. However, the uncertainties in the development of hadronic showers are much larger [18]. There are a number of possible effects which could affect

PFlow performance: the hadronic energy resolution; the transverse development of hadronic showers which will affect the performance for higher energy jets where confusion is important; and the longitudinal development of the shower which will affect both the separation of hadronic and EM showers and the amount of leakage through the rear of the HCAL. To assess the sensitivity of PFlow reconstruction to hadronic shower modelling uncertainties, five Geant4 physics lists are compared: `QGSP_BERT`, `QGS_BIC`, `FTFP_BERT`, `LHEP` and `LCPhys`. These physics lists represent a wide range of models and result in significantly different predictions for total energy deposition, and the longitudinal and transverse shower profiles. For each Physics list, the calibration constants in PandoraPFA are re-tuned, but no attempt to re-optimise the algorithm is made. The jet energy resolutions obtained are given in Table 3. Whilst non-statistical differences are seen, the rms variations are relatively small, less than about 4 %. From this study it is concluded that, for $45 - 250$ GeV jets, the jet energy resolution obtained from PFlow calorimetry as implemented in PandoraPFA does not depend strongly on the hadronic shower model.

8. Particle Flow for Multi-TeV Colliders

Given that the confusion term increases with energy, it is not *a priori* clear that PFlow calorimetry is suitable for higher energies such as $\sqrt{s} \sim 3$ TeV for the proposed CLIC collider. First studies of the potential of Particle Flow Calorimetry at CLIC were presented in [3]. For these studies the ILD concept, which is optimised for ILC energies, was modified; the HCAL thickness was increased from $6\,\lambda_I$ to $8\,\lambda_I$ and the magnetic field was increased from 3.5 T to 4.0 T. The jet energy resolution obtained for jets from $Z \to u\overline{u}, d\overline{d}, s\overline{s}$ decays at rest are listed in Table 4. For high energy jets, the effect of the increased HCAL thickness (the dominant effect) and increased magnetic field is significant. Despite the increased particle densities, the jet energy resolution (rms_{90}) for 500 GeV jets obtained from PFlow is 3.5 %. This is equivalent to $78\,\%/\sqrt{E(\mathrm{GeV})}$. This is likely to be *at least* competitive with a traditional calorimetric approach, particularly when the constant term in Equation 1 and the contribution from non-containment are accounted for. Furthermore, it should be remembered that PandoraPFA has not been optimised for such high energy jets and improvements can be expected.

Jet Energy	$\mathbf{rms_{90}}(E_{jj})/\sqrt{E_{jj}}$		$\mathbf{rms_{90}}(E_j)/E_j$	
	3.5 T & $6\,\lambda_I$	4 T & $8\,\lambda_I$	3.5 T & $6\,\lambda_I$	4 T & $8\,\lambda_I$
45 GeV	25.2 %	25.2 %	(3.74 ± 0.05) %	(3.74 ± 0.05) %
100 GeV	29.2 %	28.7 %	(2.92 ± 0.04) %	(2.87 ± 0.04) %
180 GeV	40.3 %	37.5 %	(3.00 ± 0.04) %	(2.80 ± 0.04) %
250 GeV	49.3 %	44.7 %	(3.11 ± 0.05) %	(2.83 ± 0.05) %
375 GeV	81.4 %	71.7 %	(3.64 ± 0.05) %	(3.21 ± 0.05) %
500 GeV	91.6 %	78.0 %	(4.09 ± 0.07) %	(3.49 ± 0.07) %

Table 4. Comparisons of jet energy resolutions for two sets of detector parameters. This jet energy resolution shown is for $(Z/\gamma)^* \to$uds events with $|\cos\theta_{q\overline{q}}| < 0.7$. It is expressed as: i) the effective constant α in $\mathrm{rms}_{90}(E_{jj})/E_{jj} = \alpha(E_{jj})/\sqrt{E_{jj}(\mathrm{GeV})}$, where E_{jj} is the total reconstructed energy; and ii) the fractional jet energy resolution for a single jet where $\mathrm{rms}_{90}(E_j) = \mathrm{rms}_{90}(E_{jj})/\sqrt{2}$.

8.1. Gauge Boson Mass Reconstruction

The performance of PFlow calorimetry has, up to this point, been considered in terms of the jet energy resolution from particles decaying at rest. This is appropriate for the decays of particles

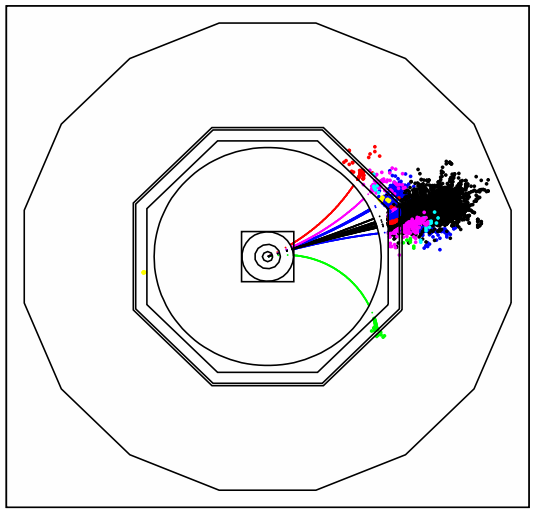

Figure 5. An example of a $Z \rightarrow d\overline{d}$ decay with $E_Z = 1\,\text{TeV}$ produced in a simulated $e^+e^- \rightarrow ZZ \rightarrow \nu\overline{\nu}d\overline{d}$ interaction in the ILD detector concept.

produced almost at rest. However, one of the goals for jet reconstruction at a future lepton collider is to be able to reconstruct gauge bosons which may be produced from the decays of BSM particles. In this case, the W/Z decays will not be at rest and the di-jet system will be boosted. At a multi-TeV lepton collider the boost may be significant. For PFlow calorimetry there are a number of effects associated with highly boosted jets: *(i)* The jet particle multiplicities are lower than those for jets of the same energy produced from decays at rest. This increases the average energy of the particles in the jet and, consequently, will result in less containment of the hadronic showers (greater leakage); *(ii)* The high jet boost decreases the average separation of the particles in the jet. This will tend to increase the confusion term; *(iii)* The two jets from the decay of a highly boosted gauge boson will tend to overlap to form a "mono-jet", as shown in Figure 5. The overlapping of jets has the potential to increase the confusion term.

Due to the likely increased confusion term, reconstructing the invariant mass of high energy gauge bosons presents a challenge for PFlow calorimetry. The PFlow reconstruction of boosted gauge bosons has been investigated by generating MC samples of $ZZ \rightarrow d\overline{d}\nu\overline{\nu}$ and $W^+W^- \rightarrow u\overline{d}\mu^-\overline{\nu}_\mu$ events at $\sqrt{s} = 0.25$, 0.5, 1.0 and 2.0 TeV. These final states give clean samples of single hadronic Z and W decays (the muons from the W decays are easy to identify and remove). The PFlow reconstructed W and Z invariant mass distributions are shown in Figure 6 and the corresponding mass resolutions are given in Table 5. A direct comparison with the jet energy resolutions of Table 4 is not straightforward due to the effects described above. However, the mass resolution (rms_{90}) of 2.8 GeV obtained from decays of gauge bosons with $E = 125\,\text{GeV}$ is compatible with that expected from the jet energy resolution of Table 4 after accounting for the gauge boson width.

For the ILC operating at $\sqrt{s} = 0.5 - 1.0\,\text{TeV}$, the typical energies of the gauge bosons of interest are likely to be in the range $E_{W/Z} = 125 - 250\,\text{GeV}$. Here the reconstructed W and Z mass peaks are well resolved. The statistical separation, which is quantified in Table 5, is approximately 2.5σ, i.e. the separation between the two peaks is approximately 2.5 times greater than the effective mass resolution.

For CLIC operating at $\sqrt{s} = 3\,\text{TeV}$, the relevant gauge boson energies are likely to be in the

$E_{W/Z}$	$\mathrm{rms}_{90}(m)$	σ_m/m	W/Z sep	ϵ
125 GeV	2.8 GeV	2.9 %	2.7σ	91 %
250 GeV	3.0 GeV	3.5 %	2.5σ	89 %
500 GeV	3.9 GeV	5.1 %	2.1σ	84 %
1000 GeV	6.4 GeV	7.0 %	1.5σ	78 %

Table 5. Invariant mass resolutions for the hadronic system in simulated $ZZ \to q\bar{q}\nu\overline{\nu}$ and $W^+W^- \to q\bar{q}\mu^-\overline{\nu}_\mu$ events in the ILD detector concept. The W/Z separation numbers, which take into account the tails, are defined such that a 2σ separation means that the optimal cut in the invariant mass distribution results in 15.8 % of events being mis-identified. The equivalent W/Z identification efficiencies, ϵ, are given in the final column. Even with infinitely good mass resolution, the best that can be achieved is 94 % due to the tails of the Breit-Wigner distribution and, thus, the possible range for ϵ is $50 - 94$ %;

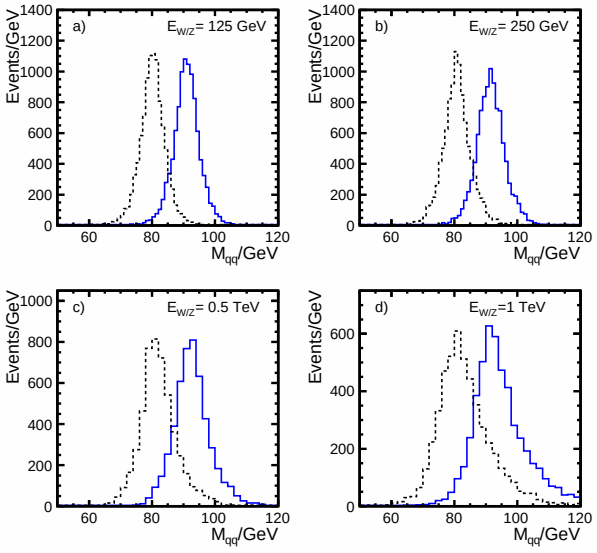

Figure 6. Reconstructed invariant mass distributions for the hadronic system in simulated $ZZ \to q\bar{q}\nu\overline{\nu}$ and $W^+W^- \to q\bar{q}\mu^-\overline{\nu}_\mu$ events as simulated in the modified ILD detector model.

range $0.5 - 1.0$ TeV. At the low end of this range there is reasonable separation (2.1σ) between the W and Z peaks. Even for 1 TeV W/Z decays, where the events mostly appear as a single energetic mono-jet, the mass resolution achieved by the current version of PandoraPFA allows separation between W and Z decays at the 1.5σ level. However, it should be remembered that PandoraPFA has not been optimised for such high energy jets, and these results represent a lower bound on what can be achieved. Since Calor 2010 progress has been made in this area. From this study it is concluded that PFlow calorimetry is certainly not ruled out for a multi-TeV lepton collider. Particle flow reconstruction may be particularly well adapted to the determination of the masses of highly boosted system which appear as mono-jets, where the resolution of the structure within the jet is essential to obtain a good mass resolution.

9. Conclusions

A sophisticated particle flow reconstruction algorithm, PandoraPFA, has been developed to study the potential of high granularity Particle Flow calorimetry at a future linear collider.

The algorithm incorporates a number of techniques, e.g. topological clustering and statistical reclustering, which take advantage of the highly segmented calorimeters being considered for the ILC and beyond. Using this algorithm it has been demonstrated that Particle Flow Calorimetry can meet the ILC requirements for jet energy resolution. For jets in the energy range $40 - 400\,\mathrm{GeV}$, the jet energy resolution, σ_E/E, is better than $4\,\%$. This conclusion does not depend strongly on the details of the modelling of hadronic showers. First studies of particle flow calorimetry for a multi-TeV collider such as CLIC show considerable promise. A jet energy resolution below $4\,\%$ is achievable for jets with energies less than approximately $600\,\mathrm{GeV}$. Reasonable separation of the hadronic decays of W and Z bosons is achievable for W/Z energies of up to approximately $1\,\mathrm{TeV}$.

In conclusion, since Calor 2008, our understanding of the potential of particle flow calorimetry has increased; it provides a technologically feasible route to achieving unprecedented jet energy resolution at a future lepton collider and as such form the current baseline for ILC and CLIC detector concepts. It should be remembered that the current PandoraPFA algorithm is still evolving and significant improvements in resolution are anticipated, particularly for higher energy jets.

10. Acknowledgements

I would like to thank the organisers of Calor 2010 for arranging such a stimulating and enjoyable conference. I would like to acknowledge the UK Science and Technology Facilities Council (STFC) for the continued support of this work. I would also like to thank colleagues in the CALICE collaboration and those working on the ILD detector concept for providing the high quality simulation and software frameworks used for the studies described in these proceedings.

References

[1] J.-C. Brient and H. Videau, "The calorimetry at a future e^+e^- linear collider", arXiv:hep-ex/0202004.
[2] V. L. Mogunov, "Energy-flow Method for Multi-jet Effective Mass Reconstruction in the Highly Granular TESLA Calorimeter", proceedings of the Snowmass Summer Study on the Future of Particle Physics, Snowmass, U.S.A. (2001).
[3] M. Thomson, Nucl. Instr. and Meth. **A611** (2009) 25.
[4] International Linear Collider reference design report. 1: Executive summary. 2: Physics at the ILC. 3: Accelerator. 4: Detectors, J. Brau (ed.), *et al.*, ILC-REPORT-2007-001 (2007).
[5] ALEPH Collaboration, D. Buskulic et al., Nucl. Instr. and Meth. **A360** (1995) 481.
[6] F. Gaede, Nucl. Instr. and Meth. **A559** (2006) 177.
[7] GEANT4 collaboration, S. Agostinelli *et al.*, Nucl. Instr. and Meth. **A506** (2003) 3;
GEANT4 collaboration, J. Allison *et al.*, IEEE Trans. Nucl. Sci. 53 (2006) 1.
[8] ILD Letter of Intent, arXiv:1006.3396.
[9] J. C. Brient, *et al.*, "CALICE Report to the R&D Review Panel", ILC-DET-2007-024 (2007); arXiv:0707.1245.
[10] T. Behnke, *et al.*, "Track Reconstruction for a Detector at TESLA", LC-DET-2001-029 (2001), and references therein.
[11] DELPHI Collaboration, DELPHI Data Analysis Program (DELANA) User's Guide, DELPHI 89-44 PROG 137 (1989).
[12] M. A. Thomson, "Progress with Particle Flow Calorimetry", Proceedings of LCWS2007, DESY, Hamburg, June 2007. arXiv:0709.1360.
[13] T. Sjöstrand, Comp. Phys. Comm. **135** (2001) 238.
[14] OPAL Collaboration, G. Alexander *et al.*, Z. Phys. **C69** (1996) 543.
[15] CALICE Collaboration, C. Adloff *et al.*, accepted for publication by NIMA (2009); arXiv:0811.2354.
[16] "Linear Collider Physics List",
http://www.slac.stanford.edu/comp/physics/geant/slac_physics_lists/ilc/ilc_physics_list.html
[17] R. Wigmans, Calor 2010.
[18] R. Wigmans, Proc. of HSW06, Fermilab, 2006, AIP Conf. Proc. 896 (2007) 123.
[19] G. Guignard (ed.), *et al.*, "A 3 TeV Linear Collider Based on CLIC Technology", CERN-2000-008 (2000).